IEEE Access
Multidisciplinary | Rapid Review | Open Access Journal

Received 16 July 2022, accepted 19 August 2022, date of publication 23 August 2022, date of current version 19 September 2022.

Digital Object Identifier 10.1109/ACCESS.2022.3201131

RESEARCH ARTICLE

Robust Bounded Control Design and Experimental Verification for Permanent Magnet Linear Motor With Inequality Constraints

SHENGCHAO ZHEN[1,2], (Member, IEEE), MENG ZHANG[1,2], XIAOLI LIU[1,2], HAN ZHAO[1,2], YE-HWA CHEN[3,4], (Member, IEEE), AND XIAOFEI CHEN[1,2]

[1]School of Mechanical Engineering, Hefei University of Technology, Hefei 230009, China
[2]Anhui Key Laboratory of Digital Design and Manufacturing, Hefei University of Technology, Hefei 230009, China
[3]George W. Woodruff School of Mechanical Engineering, Georgia Institute of Technology, Atlanta, GA 30332, USA
[4]Key Laboratory of Road Construction Technology and Equipment of MOE, Chang'an University, Xi'an 710064, China

Corresponding authors: Xiaoli Liu (xiaolihfut@qq.com) and Xiaofei Chen (492486492@qq.com)

This work was supported in part by the National Natural Science Foundation of China under Grant 52175083; in part by the Fundamental Research Funds for the Central Universities under Grant PA2021KCPY0035; in part by the Key Laboratory of Construction Hydraulic Robots of Anhui Higher Education Institutes, Tongling University, under Grant TLXYCHR-O-21ZD01; in part by the University Synergy Innovation Program of Anhui Province under Grant GXXT-2021-010; in part by the Key Research and Development Program of Anhui Province under Grant 2022a05020014; in part by the Pioneer Program Project of Zhejiang Province under Grant 2022C03018; and in part by the Robot Research Laboratory Construction Project of West Anhui University under Grant 21AT01046807142.

ABSTRACT The robust bounded control problem for the permanent magnet linear motors with inequality constraints is studied. Firstly, the dynamical model of the system is built, through the state transformation is used to satisfy the inequality constraint of the position output. Thus, the controller after the state transformation can ensure that the control output of the linear motor stays the desired range. Selecting the appropriate boundary function, and then the upper and lower bounds of the control output can be set according to our control requirements. The control scheme can guarantee uniform boundedness and uniform ultimate boundedness. The results of experiments and simulation show that the proposed algorithm can assure the control output within the desired range regardless of the uncertainty.

INDEX TERMS State transformation, inequality constraints, robust control, linear motor, uncertainty.

I. INTRODUCTION

The permanent magnet linear motor (PMLM) has simple structure, high execution efficiency and fast response speed [1], [2]. It has been widely used in the field of intelligent manufacturing and industrial production [3], [4]. The principle of PMLM is equivalent to the rotating motor, which is equivalent to expanding the rotating motor into a straight line. Both of them use three-phase coil windings and realize the steering function of the motor through the internal Hall element. Because the linear motor is directly connected to the load, there is no need for gear, belt, and other transmission links. This linear motor can reduce friction and interference [5], [6]. And it can avoid mechanical lag, return error, and other defects of the rotating motor. Theoretical travel is not limited. Therefore, the permanent magnet linear motor can satisfy the needs of high speed, high dynamic response, and high precision when driving directly. In addition, the control performance of PMLM is also influenced by all kinds of uncertain factors, such as uncharted external disturbance, friction [7], etc. In the study of PMLM, it is essential to improve the control performance [8], [9].

In the control technology of PMLM, the precise control of linear motors is essential [10], but the influence of unknown external disturbance and friction increases the difficulty of linear motor position control. [11] designed a robust controller composed of adaptive compensator, PID feedback controller and feedforward compensator. [12] and [13] proposed a typical adaptive robust control, which combines robust control and traditional adaptive control to overcome various

The associate editor coordinating the review of this manuscript and approving it for publication was Shuai Liu.

uncertainties. [14] proposed a robust position tracking control method of PMLM based on model. [15] designed a controller combining adaptive robustness and neural network, which has a certain anti-interference ability. [16] and [17] proposes a robust visual tracking method based on fuzzy detection strategy. [18] proposes an improved PID control or redesigned robust control with simple implementation and practical results. [19] designed a robust approximate constraint controller based on the Udwadia-Kalaba equation to control PMLM. For the effect of nonlinear factors, [20] proposes an adaptive compensation controller. These resolve the unknown load and friction effect of the permanent magnet linear motor to a certain extent. However, under actual working conditions, the displacement of permanent magnet linear motor must be limited within a certain range [21], [22]. [23] designed a controller considering input constraints and parameter uncertainties for nonholonomic wheeled mobile robot. [24] proposed a trajectory planning approach to achieve minimum energy consumption and zero residual vibration for flexible servomotor systems with state constraints. [25] studied the adaptive neural torsional vibration suppression control problem for the drive system with state and input constraints. Because the travel of the linear motor has a range, when the motor is subjected to external interference, the displacement of the linear motor deviates from the predetermined trajectory, the bumping phenomenon will occur, which will not only have a certain impact on the lifetime and accuracy of the motor, but also may cause production accidents. Whether this condition can be satisfied is closely related to product safety issues.

So far, few literatures have considered the problem of bilateral constrained control for linear motors. The research scope of this paper belongs to the PMLM technology. Trajectory tracking control for nonlinear linear motors with uncertain external disturbances is studied. There are uncertainties in the system, which may be caused by external load disturbance and unknown parameters. Other than its possible boundary, no other information is known. This is a problem with bounded control output. Because PMLM has a lower and an upper limit, the displacement of the PMLM needs to be limited to the desired range.

From the analysis of the existing literature, it can be seen that there are some problems in the control of PMLM. From the perspective of these difficulties, the main contributions of this paper are three aspects. Firstly, aiming at the bounded control of PMLM, a method of the state transformation is proposed, which can transform the bounded state into the unbounded state. Secondly, the robust bounded controller of permanent magnet linear motor with inequality constraints is proposed to control the transformed system under the conditions of uncertainties. The uniform boundedness and uniform ultimate boundedness of uncertain systems are proved. Finally, the numerical simulation and experimental verification of the PMLM are completed. Through the analysis of the experimental and simulation results, it is shown that the proposed robust control with inequality constraints can ensure the performance of the PMLM mechanical system under the conditions of uncertainties. And the displacement of permanent magnet linear motor system can be controlled within the defined range. The effect of control can meet the requirements of some high applications.

II. DYNAMIC MODEL OF PMLM

A complete PMLM system includes cushion, linear motor, displacement sensor, guide rail, and drag chain, etc [26]. The cushion is used to prevent the motor body from being damaged when the moving parts of the linear motor move back and forth. And the displacement sensor is used to detect the position of the motor in real time.

For PMLM, its dynamic model is usually approximated by a second-order system [27], which can be expressed by equation(1).

$$\begin{cases} \dot{y}_1(t) = y_2(t) \\ \dot{y}_2(t) = -\dfrac{k_f k_e}{Rm} y_2(t) + \dfrac{k_f}{Rm} v(t) - \dfrac{d(t)}{m} \\ x(t) = y_1(t) \end{cases} \tag{1}$$

Here, y_1 represents the moving displacement of the linear motor, $y_1 \in (y_m, y_M)$, y_m represents the lower bound of displacement and y_M represents the upper bound of displacement. y_2 represents the linear velocity of PMLM, R represents the impedance, m represents the mass of the motor, k_f represents the power constant, k_e represents the back electromotive force, and $d(t)$ can be regarded as the disturbance including ripple force and friction force. $v(t)$ is the control signal.

It is assumed that the disturbance of the motor consists of two terms, namely the friction force and the ripple force, and friction varies with load. It is expressed as follows

$$d(t) = F_{ripple} + F_{fric} \tag{2}$$

Here, F_{ripple} is the ripple force,F_{fric} is the friction force. F_{fric} is expressed by the equation(3)

$$F_{fric} = \left[f_c + (f_s - f_c)\, e^{-(\dot{y}/\dot{x}_s)^2} + f_v \dot{y} \right] sign(\dot{y}) \tag{3}$$

where f_c represents the Coulomb friction coefficient, f_s represents the static friction coefficient, f_v represents the viscous friction coefficient, x_s represents the lubricant parameter [28]. Here We use the overall identification method based on the least squares to obtain friction parameters.

F_{ripple} is described as:

$$F_{ripple} = A_1 \sin(\omega y) + A_2 \sin(3\omega y) + A_3 \sin(5\omega y) \tag{4}$$

Here A_1, A_2, A_3, ω are constants.

We choose y as the generalized coordinate, and y is the displacement of linear motor. We can convert the linear motor model of the approximate second-order system into the general form of the system dynamics model.

$$H(y, \sigma, t)\ddot{y}(t) + C(y, \dot{y}, \sigma, t)\dot{y}(t) + F(y, \dot{y}, \sigma, t) = \tau(t) \tag{5}$$

Here $t \in R$ represents the time, $y \in R^n$ represents the coordinate, $\dot{y} \in R^n$ represents the velocity, $\ddot{y} \in R^n$ represents the acceleration, τ represents the control input and $\sigma \in R^p$

represents the uncertain parameter. $H(y, \sigma, t)$ represents the inertia matrix, $C(y, \dot{y}, \sigma, t)$ represents the Coriolis/centrifugal force vector, and $F(y, \dot{y}, \sigma, t)$ represents the friction force and disturbance. The functions H, C and F are continuous. Furthermore, $\Sigma \subset R^p$ is compact and unknown, which represents the possible bounding of σ.

Therefore, the dynamical model of PMLM can be expressed as follows:

$$\frac{Rm}{k_f}\ddot{y}(t) + k_e\dot{y}(t) + \frac{R}{k_f}d(t) = v(t) \tag{6}$$

Remark. In addition to the friction force, there are other uncertainties in linear motors. The mass is uncertain due to the variation of the load. Resistance usually varies with coil temperature.

Remark. Displacement y is limited within (y_m, y_M), where $y_M > y_m$, which is related to the displacement range of linear motor, when the working condition requires higher requirements. If the displacement of linear motor exceeds the defined displacement range, it may have an impact on the safety of production. However, despite the large effect, this interval condition has not been taken into account in previous studies. In the next section, we will address this problem through the state transformations.

III. THE STATE TRANSFORMATIONS

In the mechanical system of PMLM, the value of state displacement should be within the defined boundary in some applications where the working conditions are demanding. However, the existence of uncertain external disturbances in systems can cause the state variables to exceed the specified range [29]. Therefore, we propose the state transformation to convert the displacement y with limitation into the state x without limitation, which can assure that the displacement y is not able to exceed the limitation (y_m, y_M).

Assume that the motor position satisfies the bilateral constraint as follows:

$$y_m < y < y_M \tag{7}$$

Let's set the state transformation equation as:

$$x = \tan\left[\frac{\pi}{y_M - y_m}(y - y_m) - \frac{\pi}{2}\right] \tag{8}$$

with

$$x_d = \tan\left[\frac{\pi}{y_M - y_m}(y_d - y_m) - \frac{\pi}{2}\right] \tag{9}$$

Here y represents the actual position, y_d represents the expected position, x represents the actual position after the state transformation, and x_d represents the expected position after the state transformation.

Where, the constraints can be closed intervals, but other conversion functions are needed. The constraint interval in this paper is open, which is determined by the conversion function we design. Considering the practical characteristics of the linear motor, we design the conversion function as *tan* function. *tan* function is only applicable to the open interval by definition.

From the equation(8), we can see that $y \to y_M$ as $x \to +\infty$ and $y \to y_m$ as $x \to -\infty$. Thus, by selecting an appropriate function x, the state transformation can convert the state y with limitation to the state x without limitation. From equation(8), we can get

$$y = \frac{y_M - y_m}{\pi}\arctan(x) + \frac{y_M + y_m}{2} \tag{10}$$

Take the derivative of the equation(10) to get the first derivative

$$\dot{y} = \frac{y_M - y_m}{\pi}\frac{\dot{x}}{1 + x^2} \tag{11}$$

Take the derivative of the equation(11) again to get the second derivative

$$\ddot{y} = \frac{y_M - y_m}{\pi}\frac{\left[1 + x^2\right]\ddot{x} - 2x\dot{x}^2}{\left[1 + x^2\right]^2} \tag{12}$$

Substituting the equation(11) and (12) into the dynamics equation(6), we can get:

$$\frac{Rm}{k_f}\frac{y_M - y_m}{\pi}\frac{\left[1 + x^2\right]\ddot{x} - 2x\dot{x}^2}{\left[1 + x^2\right]^2} + k_e\frac{y_M - y_m}{\pi}\frac{\dot{x}}{1 + x^2} + \frac{R}{k_f}d(t) = v(t) \tag{13}$$

Further simplified to the general form of the dynamical model

$$\frac{Rm\,(y_M - y_m)\left[1 + (x)^2\right]}{\pi k_f\left[1 + (x)^2\right]^2}\ddot{x} + k_e\frac{(y_M - y_m)}{\pi\left[1 + (x)^2\right]}\dot{x} + \frac{R}{k_f}d(t) - \frac{2Rm\,(y_M - y_m)\,(x)\dot{x}^2}{\pi k_f\left[1 + (x)^2\right]^2} = v(t) \tag{14}$$

This transforms the bounded constraint problem on y into an unbounded constraint problem on x.

Accordingly, we can get the inertia matrix H, Coriolis force/centrifugal force matrix C and friction vector F of the linear motor mechanical system after the state transformation.

$$\begin{aligned} H &= \frac{Rm\,(y_M - y_m)\left(1 + x^2\right)}{k_f\pi\left(1 + x^2\right)^2} \\ C &= k_e\frac{(y_M - y_m)}{\pi\left(1 + x^2\right)} \\ F &= \frac{R}{k_f}d(t) - \frac{2Rm\,(y_M - y_m)\,x\dot{x}^2}{k_f\pi\left(1 + x^2\right)^2} \end{aligned} \tag{15}$$

(i) $H(x)$ is positive definite symmetric matrix, and is uniformly bounded for all x. It can be expressed as

$$0 < \underline{\varsigma}I \leqslant H(x) \leqslant \overline{\varsigma}I \tag{16}$$

where $\underline{\varsigma}, \overline{\varsigma}$ are positive constant.

(ii) The matrix $\dot{H}(x) - 2C(x, \dot{x})$ is skew symmetric for all $x, \dot{x}$. That is, for any vector ζ,

$$\zeta^T\{\dot{H}(x) - 2C(x, \dot{x})\}\zeta = 0 \tag{17}$$

The following figure shows the process of state transformation. The first part (a) of Figure(1) shows the ideal trajectory of the state variables. In the ideal state, $y(t)$ always stays within the bounds y_M and y_m. However, due to the uncertainty factor, the actual trajectory of $y(t)$ is shown in the second part (b). Therefore, the state transformation is applied as shown in the third part (c). Through the function α, the state variable y is converted to x. After the state transformation, y will always remain within the boundary. In the next section, a robust controller is designed to ensure that the state variable y tracks the desired trajectory.

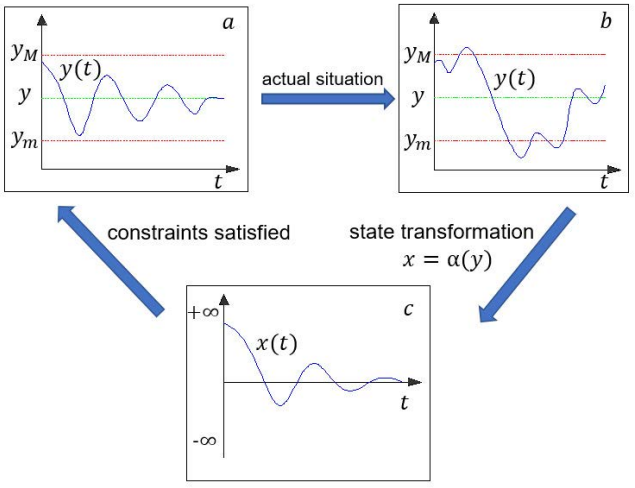

FIGURE 1. The state transformation process.

IV. ROBUST CONTROL

A. ROBUST CONTROLLER DESIGN

After the state transformations, we choose x as the generalized coordinate, where x is the state variable after the state transformation. Consider the linear motor system for position tracking control, assuming that the desired position $x^d(\cdot) : [t_0, \infty) \to R^n, x^d(\to \cdot)$ is C^2. For any given time $t \in [t_0, \infty)$, $x^d(t), \dot{x}^d(t)$ and $\ddot{x}^d(t)$ uniformly bounded. Then, the output tracking error is:

$$e(t) = x(t) - x^d(t) \tag{18}$$

and hence

$$\dot{e}(t) = \dot{x}(t) - \dot{x}^d(t), \ \ddot{e}(t) = \ddot{x}(t) - \ddot{x}^d(t) \tag{19}$$

System equation(5) can be rewritten as

$$H(x, \sigma, t)(\ddot{x}^d(t) + \ddot{e}(t)) + C(x, \dot{x}, \sigma, t)(\dot{x}^d(t) + \dot{e}(t)) + F(x, \dot{x}, \sigma, t) = \tau(t) \tag{20}$$

Actually, uncertainty exists in the system due to the uncertainty of the parameters and the constant changes of the parameters and unmodeled dynamics. Therefore, the dynamic model could be divided into the uncertain term and the nominal term. The functions $H(\cdot)$, $C(\cdot)$ and $F(\cdot)$ are expressed as follows:

$$\begin{aligned} H(x, \sigma, t) &= \Delta H(x, \sigma, t) + \overline{H}(x, t) \\ C(x, \dot{x}, \sigma, t) &= \Delta C(x, \dot{x}, \sigma, t) + \overline{C}(x, \dot{x}, t) \\ F(x, \dot{x}, \sigma, t) &= \Delta F(x, \dot{x}, \sigma, t) + \overline{F}(x, \dot{x}, t) \end{aligned} \tag{21}$$

where ΔH, ΔC and ΔF are uncertain terms which depend on σ, $\overline{H}(\cdot)$, $\overline{C}(\cdot)$ and $\overline{F}(\cdot)$ are the nominal terms.

Assuming that the boundary of uncertainty is estimated by ρ.

$$\rho(e, \dot{e}, \sigma, t) \geqslant \| \Phi(e, \dot{e}, \sigma, t) \| \tag{22}$$

where

$$\begin{aligned} \Phi(e, \dot{e}, \sigma, t) = &-\Delta H(x, \sigma, t)(\ddot{x}^d - S\dot{e}) \\ &- \Delta C(x, \dot{x}, \sigma, t)(\dot{x}^d - Se) \\ &- \Delta F(x, \dot{x}, \sigma, t) \end{aligned} \tag{23}$$

Note that for a given $S > 0$ is constant. Apparently, if all the uncertainties in the mechanical system disappear, then $\Phi \equiv 0$.

Regard the trajectory tracking error vector as follows

$$\underline{e}(t) := \left[e(t)\ \dot{e}(t)\right]^T \tag{24}$$

The problem of trajectory tracking is to design a controller to guarantee the tracking error vector $\underline{e}(t)$ small enough.

The control torque $\tau(t)$ can be geted by

$$\begin{aligned} \tau(t) = &\overline{H}(\ddot{x}^d - S\dot{e}) + \overline{C}(\dot{x}^d - Se) + \overline{F} \\ &- K_p e - K_v \dot{e} - \gamma(\dot{e} + Se)\rho^2 \end{aligned} \tag{25}$$

where K_p is the proportional control parameter and K_v is the differential control parameter. These control parameters come from traditional PID control. The scalar $\gamma > 0$. K_p, K_v and γ all are constant, which are the flexible parameter variables.

For the mechanical system expressed in equation(5), the control equation(25) adopted would make the tracking error $\underline{e}(t)$ uniformly bounded and uniformly ultimately bounded. The last item is a robust feedback item, mainly for uncertainty.

B. STABILITY ANALYSIS

Lyapunov minmax method [30], [31] is used to analyze the stability of the proposed controller. The Lyapunov function candidate [32] is choose as:

$$\begin{aligned} V(\underline{e}, t) := &\frac{1}{2}(\dot{e} + Se)^T H(e + x^d(t))(\dot{e} + Se) \\ &+ \frac{1}{2} e^T (K_p + SK_v)e \end{aligned} \tag{26}$$

In order to prove that the Lyapunov function V is a suitable candidate, V must be proved to be positive definite and decreasing.

With equation(16), $H(x, \sigma, t)$ is bounded, so

$$V \geq \frac{1}{2}\underline{\varsigma} \| \dot{e} + Se \|^2 + \frac{1}{2} e^T (K_p + SK_v)e$$

$$= \frac{1}{2}\underline{\varsigma}\left(\dot{e}^2 + 2s\dot{e}e + s^2e^2\right) + \frac{1}{2}(k_p + sk_v)e^2$$
$$= \frac{1}{2}\begin{bmatrix} e & \dot{e}\end{bmatrix}\underline{\Upsilon}\begin{bmatrix} e \\ \dot{e}\end{bmatrix} \tag{27}$$

here

$$\underline{\Upsilon} := \begin{bmatrix} \underline{\varsigma}s^2 + k_p + sk_v & \underline{\varsigma}s \\ \underline{\varsigma}s & \underline{\varsigma}\end{bmatrix} \tag{28}$$

It can be easily proved that $\underline{\Upsilon} > 0$. Therefore, V is positive definite.

$$V \geq \frac{1}{2}\lambda_{min}(\underline{\Upsilon})(e^2 + \dot{e}^2) \geq \zeta_1\|\underline{e}\|^2 \tag{29}$$

where $\zeta_1 = \min\{\frac{1}{2}\lambda_{min}(\underline{\Upsilon})\}$, $\zeta_1 > 0$.

Because the inertial matrix in equation(16) is bounded, thus

$$V \leq \frac{1}{2}\overline{\varsigma} \parallel \dot{e} + Se \parallel^2 + \frac{1}{2}e^T(K_p + SK_v)e$$
$$= \frac{1}{2}\begin{bmatrix} e\dot{e}\end{bmatrix}\overline{\Upsilon}\begin{bmatrix} e \\ \dot{e}\end{bmatrix} \tag{30}$$

where

$$\overline{\Upsilon} := \begin{bmatrix} \overline{\varsigma}s^2 + k_p + s_ik_v & \overline{\varsigma}s \\ \overline{\varsigma}s & \overline{\varsigma}\end{bmatrix} \tag{31}$$

$$V \leq \frac{1}{2}\lambda_{max}(\overline{\Upsilon})(e^2 + \dot{e}^2) \leq \zeta_2\|\underline{e}\|^2 \tag{32}$$

where $\zeta_2 = \max\{\frac{1}{2}\lambda_{max}(\overline{\Upsilon})\}$, $\zeta_2 > 0$.

Taking the time derivative of V along a trajectory of (20), for any allowed $\sigma(\cdot)$, yields

$$\dot{V} = (\dot{e} + Se)^{\mathrm{T}}H(\ddot{e} + S\dot{e}) + \frac{1}{2}(\dot{e} + Se)^{\mathrm{T}}\dot{H}(\dot{e} + Se)$$
$$+ e^T(K_p + SK_v)\dot{e} \tag{33}$$

Introduce equation(19) into the first two terms of the equation (33) denoted by $\dot{V}_s$

$$\dot{V}_s = (\dot{e} + Se)^T H(\ddot{x} - \ddot{x}^d + S\dot{e}) + \frac{1}{2}(\dot{e} + Se)^T\dot{H}(\dot{e} + Se) \tag{34}$$

Substitute $H\ddot{x}$ of equation(5) and τ of equation (25) into (34) in turn,

$$\dot{V}_s = (\dot{e} + Se)^T[(\overline{H}(\ddot{x}^d - S\dot{e}) + \overline{C}(\dot{x}^d - Se) + \overline{F}$$
$$- K_pe - K_v\dot{e} - \gamma(\dot{e} + Se)\rho^2 - C(\dot{x}^d \overbrace{-Se + Se}) + \dot{e})$$
$$- F) - H\ddot{x}^d + MS\dot{e}] + \frac{1}{2}(\dot{e} + Se)^T\dot{H}(\dot{e} + Se)$$
$$= (\dot{e} + Se)^T[-\Delta H(\ddot{x}^d - S\dot{e}) - \Delta C(\dot{x}^d - Se) -$$
$$- \Delta F - \gamma(\dot{e} + Se)\rho^2] - (\dot{e} + Se)^T(K_pe + K_v\dot{e})$$
$$+ (\dot{e} + Se)^T(\frac{1}{2}\dot{H} - C)(\dot{e} + Se) \tag{35}$$

Consider the dynamic properties of the mechanical system (17), hence

$$(\dot{e} + Se)^T(\frac{1}{2}\dot{H} - C)(\dot{e} + Se) = 0 \tag{36}$$

With equation (22)

$$\dot{V}_s = (\dot{e} + Se)^T[\Phi - \gamma(\dot{e} + Se)\rho^2] - (\dot{e} + Se)^T(K_pe$$
$$+ K_v\dot{e})$$
$$\leq (\dot{e} + Se)^T[\rho - \gamma(\dot{e} + Se)\rho^2] - \dot{e}^TK_v\dot{e} - e^TSK_pe$$
$$- e^T(K_p + SK_v)\dot{e} \tag{37}$$

Substituting equation (37) into equation (33), it is easy to get that

$$\dot{V} = (\dot{e} + Se)^T[\rho - \gamma(\dot{e} + Se)\rho^2] - \dot{e}^TK_v\dot{e} - e^TSK_pe$$
$$\leq \frac{1}{4\gamma} - \zeta_3\left\|\underline{e}(t)\right\|^2 \tag{38}$$

for all $(\underline{e}, t) \in R^{2n} \times R$, where

$$\zeta_3 = \min\{\lambda_{min}(K_v), \lambda_{min}(SK_p)\} \tag{39}$$

The uniform boundedness performance follows. Upon invoking the standard arguments as in [33], that is, given any $r > 0$ with $\left\|\underline{e}(t_0))\right\| \leq r$, where t_0 is the initial time, there is a $d(r)$ given by

$$d(r) = \begin{cases} \sqrt{\frac{\zeta_2}{\zeta_1}}\, r, & \text{if } r > R \\ \sqrt{\frac{\zeta_2}{\zeta_1}}\, R, & \text{if } r \leq R \end{cases} \tag{40}$$

$$R = \frac{1}{2\gamma}\sqrt{\frac{1}{\zeta_3}} \tag{41}$$

such that $\left\|\underline{e}\right\| \leq d(r)$ for all $t \geq t_0$.

Furthermore, uniform ultimate boundedness also follows. That is $\left\|\underline{e}\right\| \leq \overline{d}, \forall t \geq t_0 + T(\overline{d}, r)$, with

$$\overline{d} > \underline{d} = \sqrt{\frac{\zeta_2}{\zeta_1}}\, R \tag{42}$$

$$T(\overline{d}, r) = \begin{cases} 0 & \text{if } r \leq \overline{d}\sqrt{\frac{\zeta_1}{\zeta_2}} \\ \frac{\zeta_2 r^2 - (\zeta_1{}^2/\zeta_2)\overline{d}^2}{\zeta_3(\zeta_1/\zeta_2)\overline{d}^2 - \frac{1}{4\gamma}} & \text{if } r > \overline{d}\sqrt{\frac{\zeta_1}{\zeta_2}} \end{cases} \tag{43}$$

Please note that by adjusting the parameter variables K_p, K_v and γ from equation (41), $\overline{d}$ can become arbitrarily small.

C. DESIGN PROCEDURE

As shown in Figure(2), we summarize the flow chart of robust bounded control with inequality constraints for PMLM. In this paper, the dynamical system satisfying the output state with inequality constraint for the linear motor is obtained. By selecting an appropriate transformation function, the output state y with limitation is transformed into the state x without limitation. Then we have robust control over the unbounded state x. No matter how the uncertain external disturbance is, the control output y can be kept within the controllable and safe range. For the transformed state x, we designed a robust controller based on PD. By selecting proper K_p, K_v, γ, and S, the error of linear motor trajectory tracking is small enough. As K_p increases, the system response speeds up, and the steady-state error decreases.

However, as K_p increases, the system gradually overshoots and oscillates at the same time, and the system takes longer to reach steady state, and the control cost is higher. The introduction of K_v can reduce the overregulation caused by K_p, which makes the response of the whole system slower and the steady-state error larger. In addition, the value of γ directly affects the ultimately bounded range and determines the trade-off between system performance and control cost. And S is closely related to the convergence rate of the error.

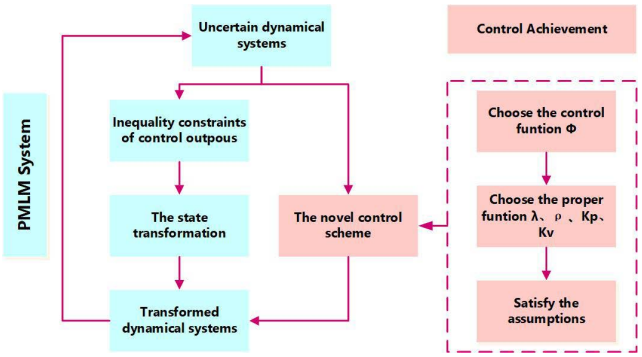

FIGURE 2. The control design procedure.

V. SIMULATION AND EXPERIMENTAL RESULTS

Next, we will use numerical simulation and experiments on the permanent magnet linear motor to verify the correctness of the robust bounded control theory with inequality constraints. The parameters of the PMLM are shown in Table 1.

TABLE 1. The parameters of the PMLM.

Notation	Value	Definition	Unit
M	$\overline{M} = 1.4$	Mass of the liner otor	kg
R	$\overline{R} = 5.6$	Resistance of the system	$ohms$
k_f	$\overline{k}_f = 1$	Force constant	N/A
k_e	$\overline{k}_e = 60$	Back electromotive force	$V/m/s$
f_v	5	Viscous friction coefficient	$N/m/s$
f_s	8	Static friction coefficient	N
f_c	5	Coulomb friction coefficient	N
$\dot{x_s}$	0.5	Lubricant parameter	m/s
A_1	3	The proportion of coefficient	–
A_2	2	The proportion of coefficient	–
A_3	1	The proportion of coefficient	–

A. NUMERICAL SIMULATION

Firstly, we use the MATLAB to verify the correctness of the robust bounded control theory for permanent magnet linear motor with inequality constraints. We use the step signal and sinusoidal signal to study the ability, which dealing with uncertainty and dynamic characteristics of the robust controller with and without inequality constraints. For the simulation, we select the appropriate controller parameters as follows, $K_p = 100$; $K_v = 10$; $S = 1$; $\gamma = 0.6954$; Quality is treated as an uncertainty, $\Delta M = 5sin(0.01t)$. The initial value of sinusoidal tracking is $e(0) = \begin{bmatrix}0.05 & 0\end{bmatrix}^T$. We set motor position x limited to $[-0.101m, 0.101m]$

We present the step signal as shown below:

$$x = 0.1\ m \tag{44}$$

We present the sinusoidal signal, which enables the permanent magnet linear motor system to achieve sinusoidal trajectory tracking. We present the sine signal as shown below:

$$x = 0.1sin(\frac{t}{4})m \tag{45}$$

We analyze the results of the step signal response. The comparison of response between the robust controller with and without inequality constraints to control the PMLM system is shown in Figure 3. The step response of the linear motor without the inequality constraint reaches stability at approximately 0.01 s. The overshoot of the step response is 102.8 mm, which exceeds the set upper bound ($101mm$) by 1.8 mm. The step response of the linear motor with the inequality constraint reaches stability at 0.15 s, and the maximum value during the response is $100mm$, which does not exceed the set upper bound ($101mm$).

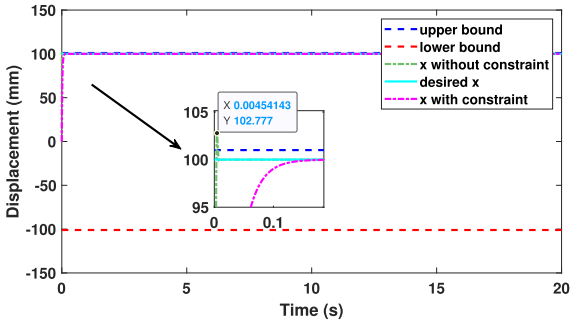

FIGURE 3. Comparison of tracking the step signal with and without inequality constraints.

Next, we analyze the simulation results of the sinusoidal signal response. The comparison of response between the robust controller with and without inequality constraints to control the PMLM is shown in Figure 4. The errors of sinusoidal trajectory tracking are shown in Figure 5. The comparison of the control inputs is shown in Figure 6.

As can be seen from Figure 4, the initial displacement of the linear motor is $50mm$, which satisfies the condition that the initial value is incompatible. The linear motor without the inequality constraint reaches stability at $2s$ when tracking the sinusoidal curve. The maximum overshoot of the sinusoidal tracking is $102mm$, which exceeds the set upper bound $101mm$. The sine tracking of the linear motor with inequality constraint reaches stability at 0.2 s. The boundary condition is not exceeded and the error range is controlled within $[-0.02\ mm, 0.02\ mm]$. From the simulation results, it can be seen that the control effect with the inequality constraint is significantly better than the effect without the inequality constraint.

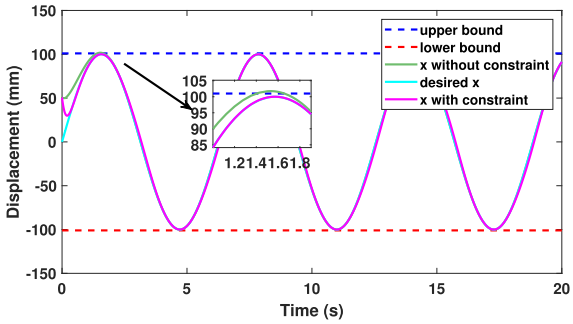

FIGURE 4. Comparison of tracking the sinusoid signal with and without inequality constraints.

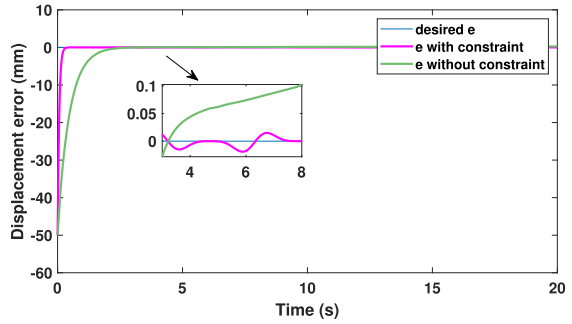

FIGURE 5. The error of tracking a sinusoid signal with and without inequality constraints.

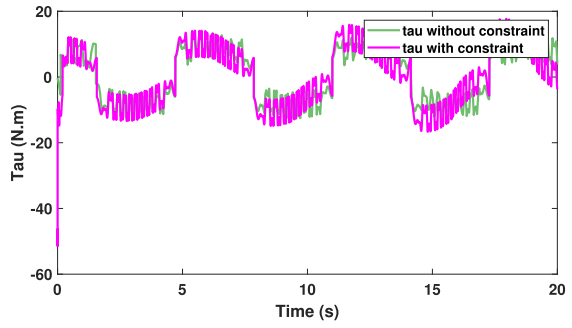

FIGURE 6. The current of tracking a sinusoid signal with and without inequality constraints.

B. RESULTS OF PMLM EXPERIMENT

In this section, we will carry out the experimental verification of the inequality constraint algorithm on the experimental platform of PMLM. Figure 7 shows our experimental platform, which primarily consists of the following parts: cSPACE control platform, PMLM mechanical systems, and computer with MATLAB/Simulink simulation software. We will use the control block diagram of Simulink to complete the experiment. Combined with numerical simulation, two groups of experiments are designed: step response and sinusoidal signal trajectory tracking. For the trajectory tracking problem of the sinusoidal signal, some interference is applied to the motor in the process of moving to test the motor's ability to deal with the uncertainty and verify the correctness and practicability of the robust controller with

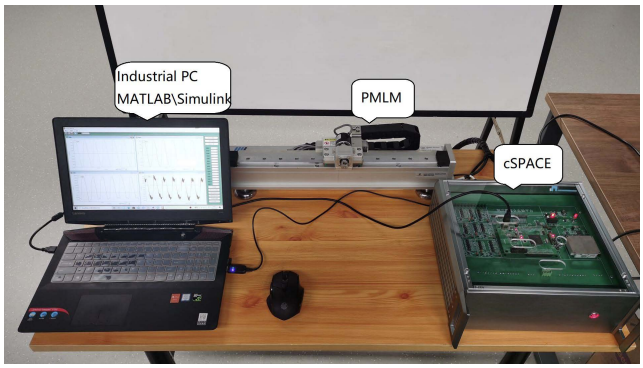

FIGURE 7. Permanent magnet linear motor(PMLM) experimental platform.

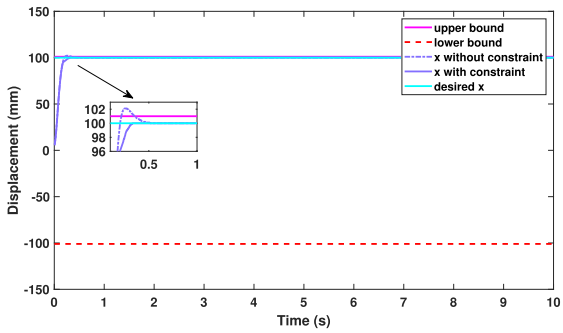

FIGURE 8. The experimental results of tracking a step signal with and without inequality constraints.

inequality constraints. Here, the resistance and inductance will tend to become larger to some extent with increasing temperature. But these changes are negligible and are not considered in this paper at this time. We select the appropriate controller parameters as follows, $K_p = 120$; $K_v = 10$; $S = 1$; $\gamma = 0.6954$.

Figure 8 shows the step responses of PMLM with and without inequality constraints. We can see that in the experiment of step response, The step time without the inequality constraint is $1s$ to reach stability. The maximum value during the step response is $102mm$, which exceeds the set upper bound $101mm$. The step response with inequality constraint reaches stability at $0.8\ s$, and the maximum value during the response is close to $100mm$. So the robust controller with inequality constraints can limit the motor displacement within the boundary.

The sinusoidal trajectory tracked by the linear motor is $x = 0.095sin(\frac{t}{4})m$. The sinusoidal trace of the robust controller without inequality constraints is shown in Figure 9. In the sinusoidal tracking experiment without inequality constraint, the artificial external disturbances are applied at 7s,9s,11s,13s, respectively. We can clearly see that when the motor is controlled by a robust controller without inequality constraints, the displacement of the linear motor reaches the minimum value $-106mm$ and maximum value $105mm$ at 11s and 13s respectively, which exceed the set

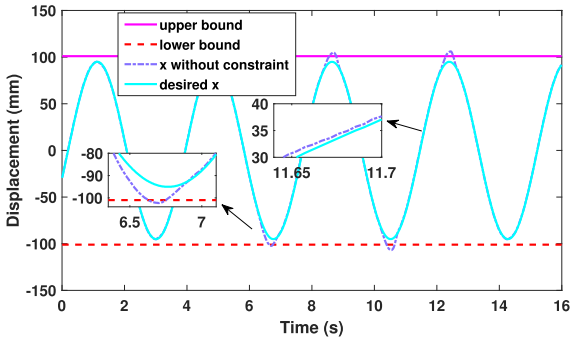

FIGURE 9. The experimental results of tracking sinusoidal signals without inequality constraints.

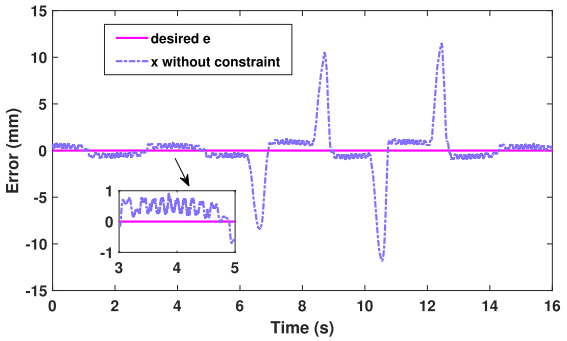

FIGURE 10. The experimental error results of tracking sinusoidal signals without inequality constraints.

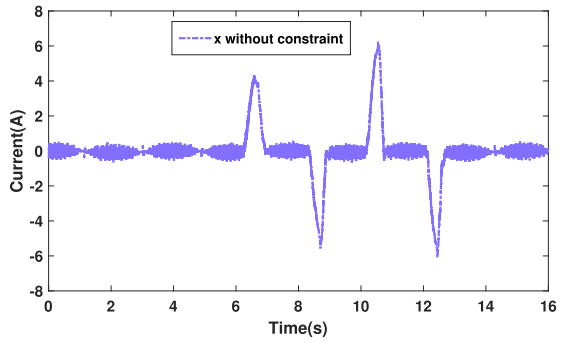

FIGURE 11. The experimental current results of tracking sinusoidal signals without inequality constraints.

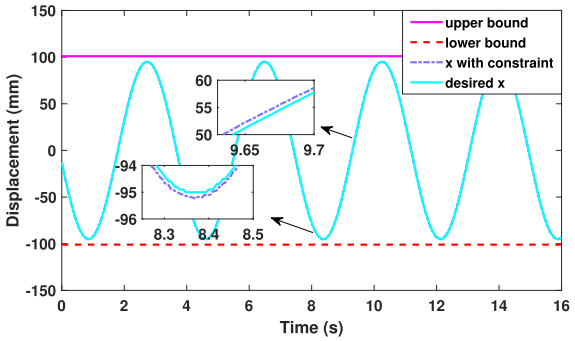

FIGURE 12. The experimental results of tracking sinusoidal signals with inequality constraints.

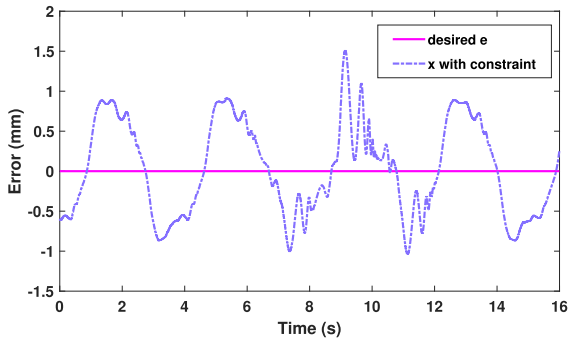

FIGURE 13. The experimental error results of tracking sinusoidal signals with inequality constraints.

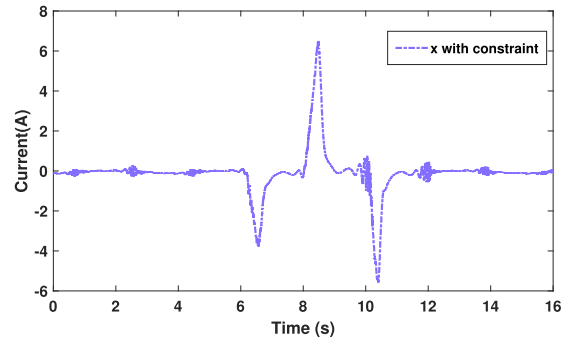

FIGURE 14. The experimental current results of tracking sinusoidal signals with inequality constraints.

boundary $[-101\ mm,\ 101\ mm]$. As can be seen from Figure 10, the trajectory tracking error of the robust controller without the inequality constraint varies in $[-0.93\ mm,\ 0.93\ mm]$ when it reaches stability. When external disturbances are applied, the maximum and minimum errors of the linear motor are $[-11.83\ mm,\ 11.83\ mm]$. Control torque of the filtered PMLM is shown in Figure 11.

The sinusoidal trace of the robust controller with inequality constraints is shown in Figure 12. In the sinusoidal tracking experiment with inequality constraint, the artificial external disturbances are applied at 7s,9s,11s, respectively. We can clearly see that when the motor is controlled by a robust controller with inequality constraints, the displacement is always controlled within the set boundaries $[-101\ mm,\ 101\ mm]$. As can be seen from Figure 13, the trajectory tracking error of the robust controller with the inequality constraint varies in $[-0.5\ mm,\ 0.5\ mm]$ when it reaches stability. When external disturbances are applied, the maximum and minimum errors of the linear motor are $[-0.985\ mm,\ 0.985\ mm]$. Control torque of the filtered PMLM is shown in Figure 14.

Here, we uses RMSE and MAXE to illustrate the impact of algorithms with and without inequality constraints on dynamic performance, where

$$MAXE = max\ (|e_i|) \tag{46}$$

$$RMSE = \sqrt{\frac{1}{N}\sum_{i=1}^{N} e_i^2} \tag{47}$$

From Figure 15, We can clearly see that the control performance of the robust controller without the inequality constraint is comparable to the robust controller with the inequality at steady state. However, when there is an external disturbance, the performance of the robust controller with inequality constraint is much better than that of the robust controller without inequality constraint. And the position of the linear motor can be strictly restrained within the set boundaries to prevent the occurrence of edge-bumping and production accidents.

The sinusoidal experiment results show that the proposed inequality constraint theory can improve the ability of the robust controller to deal with some uncertainties such as external disturbance and friction.

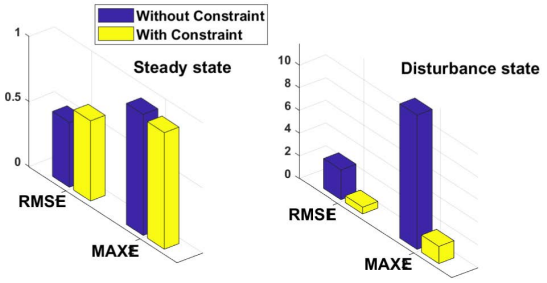

FIGURE 15. Experiment result of tracking sinusoidal signal.

VI. CONCLUSION

In this paper, a robust bounded control algorithm for permanent magnet linear motors with inequality constraints is proposed. Based on the state transformation, the algorithm transforms the state variable domain to satisfy the inequality constraint of the control output. A robust bounded controller is designed, which consists of a model-based PD control item and robust item. Lyapunov minimax method is used to prove the effectiveness of the algorithm.

The simulation and experimental results of the PMLM experimental platform based on cSPACE show that the proposed robust controller with inequality constraint can be used to control the PMLM, which can be used to limit the displacement of the PMLM within the set limit during the process of robust control. The proposed inequality constraint theory can improve the ability of a robust controller to deal with external disturbance, friction, and other uncertainties, which is especially suitable for practical engineering applications. Next, we will take the motor temperature compensation into consideration to further reduce the effect of temperature variation on inductance and resistance. And we will verify the proposed control algorithm on other uncertain systems, such as the two-link manipulator and the permanent magnet synchronous motor.

REFERENCES

[1] J. Kim, S. Choi, K. Cho, and K. Nam, "Position estimation using linear Hall sensors for permanent magnet linear motor systems," *IEEE Trans. Ind. Electron.*, vol. 63, no. 12, pp. 7644–7652, Dec. 2016.

[2] K. K. Tan, S. N. Huang, and T. H. Lee, "Robust adaptive numerical compensation for friction and force ripple in permanent-magnet linear motors," *IEEE Trans. Magn.*, vol. 38, no. 1, pp. 221–228, Jan. 2002.

[3] S.-L. Chen, K. K. Tan, S. Huang, and C. S. Teo, "Modeling and compensation of ripples and friction in permanent-magnet linear motor using a hysteretic relay," *IEEE/ASME Trans. Mechatronics*, vol. 15, no. 4, pp. 586–594, Aug. 2009.

[4] Y. Ma, G. Yang, Q. Sun, X. Wang, and Q. Sun, "Adaptive robust control for tank stability: A constraint-following approach," *Proc. Inst. Mech. Eng., I, J. Syst. Control Eng.*, vol. 235, no. 1, pp. 3–14, Jan. 2021.

[5] H. Li, M. D. Le, Z. M. Gong, and W. Lin, "Motion profile design to reduce residual vibration of high-speed positioning stages," *IEEE/ASME Trans. Mechatronics*, vol. 14, no. 2, pp. 264–269, Apr. 2009.

[6] L. Xu and B. Yao, "Adaptive robust precision motion control of linear motors with negligible electrical dynamics: Theory and experiments," *IEEE/ASME Trans. Mechatronics*, vol. 6, no. 4, pp. 444–452, Dec. 2001.

[7] T. Hu, W. Xue, and Y. Huang, "Active disturbance rejection control for permanent magnet linear motor," in *Proc. 31st Chin. Control Conf.*, Jul. 2012, pp. 296–301.

[8] M.-T. Yan and Y.-J. Shiu, "Theory and application of a combined feedback–feedforward control and disturbance observer in linear motor drive wire-EDM machines," *Int. J. Mach. Tools Manuf.*, vol. 48, nos. 3–4, pp. 388–401, Mar. 2008.

[9] K. K. Tan, T. H. Lee, H. F. Dou, S. J. Chin, and S. Zhao, "Precision motion control with disturbance observer for pulsewidth-modulated-driven permanent-magnet linear motors," *IEEE Trans. Magn.*, vol. 39, no. 3, pp. 1813–1818, May 2003.

[10] M.-T. Yan and T.-H. Cheng, "High accuracy motion control of linear motor drive wire-EDM machines," *Int. J. Adv. Manuf. Technol.*, vol. 40, nos. 9–10, pp. 918–928, Feb. 2009.

[11] K. K. Tan, S. N. Huang, H. F. Dou, T. H. Lee, S. J. Chin, and S. Y. Lim, "Adaptive robust motion control for precise trajectory tracking applications," *ISA Trans.*, vol. 40, no. 1, pp. 57–71, Jan. 2001.

[12] B. Yao, C. X. Hu, L. Lu, and Q. F. Wang, "Adaptive robust precision motion control of a high-speed industrial gantry with cogging force compensations," *IEEE Trans. Control Syst. Technol.*, vol. 19, no. 5, pp. 1149–1159, Sep. 2011.

[13] H.-J. Ahn, K. Hwang, and D. C. Nguyen, "Eddy current damper for passive reaction force compensation of a linear motor motion stage," *Proc. Inst. Mech. Eng., I, J. Syst. Control Eng.*, vol. 231, no. 5, pp. 360–366, May 2017.

[14] X. Liu, S. Zhen, H. Zhao, H. Sun, and Y.-H. Chen, "Fuzzy-set theory based optimal robust design for position tracking control of permanent magnet linear motor," *IEEE Access*, vol. 7, pp. 153829–153841, 2019.

[15] Z. Wang, C. Hu, Y. Zhu, S. He, K. Yang, and M. Zhang, "Neural network learning adaptive robust control of an industrial linear motor-driven stage with disturbance rejection ability," *IEEE Trans. Ind. Informat.*, vol. 13, no. 5, pp. 2172–2183, Oct. 2017.

[16] S. Liu, S. Wang, X. Liu, C.-T. Lin, and Z. Lv, "Fuzzy detection aided real-time and robust visual tracking under complex environments," *IEEE Trans. Fuzzy Syst.*, vol. 29, no. 1, pp. 90–102, Jan. 2021.

[17] S. Liu, C. Guo, F. Al-Turjman, K. Muhammad, and V. H. C. de Albuquerque, "Reliability of response region: A novel mechanism in visual tracking by edge computing for IIoT environments," *Mech. Syst. Signal Process.*, vol. 138, Apr. 2020, Art. no. 106537.

[18] X. Liu, S. Zhen, H. Sun, and H. Zhao, "A novel model-based robust control for position tracking of permanent magnet linear motor," *IEEE Trans. Ind. Electron.*, vol. 67, no. 9, pp. 7767–7777, Sep. 2020.

[19] K. Huang, M. Wang, H. Sun, and S. Zhen, "Robust approximate constraint-following control design for permanent magnet linear motor and experimental validation," *J. Vib. Control*, vol. 27, nos. 1–2, pp. 119–128, Jan. 2021.

[20] Y. Li, L. Zheng, Y. Liang, and Y. Yu, "Adaptive compensation control of an electromagnetic active suspension system based on nonlinear characteristics of the linear motor," *J. Vib. Control*, vol. 26, nos. 21–22, 2020, Art. no. 107754632090998.

[21] J. Xu, Y.-H. Chen, and H. Guo, "Robust levitation control for maglev systems with guaranteed bounded airgap," *ISA Trans.*, vol. 59, pp. 205–214, Nov. 2015.

[22] R. Zhao, Y.-H. Chen, and S. Jiao, "Optimal design of robust control for positive fuzzy dynamic systems with one-sided control constraint," *J. Intell. Fuzzy Syst.*, vol. 32, no. 1, pp. 723–735, Jan. 2017.

[23] Z. Wang, G. Li, X. Chen, H. Zhang, and Q. Chen, "Simultaneous stabilization and tracking of nonholonomic WMRs with input constraints: Controller design and experimental validation," *IEEE Trans. Ind. Electron.*, vol. 66, no. 7, pp. 5343–5352, Jul. 2019.
[24] H. Mu, H. Chen, and Y. Zhu, "Vibration-energy-optimal trajectory planning for flexible servomotor systems with state constraints," *IET Control Theory Appl.*, vol. 13, no. 1, pp. 59–68, Jan. 2019.
[25] C. Qian, C. Hua, L. Zhang, and Z. Bai, "Adaptive neural torsional vibration suppression of the rolling mill main drive system subject to state and input constraints with sensor errors," *J. Franklin Inst.*, vol. 357, no. 17, pp. 12886–12903, Nov. 2020.
[26] G. Li, X. Wang, X. Xu, and J. Liu, "Electromagnetic characteristics analysis of primary permanent magnet linear motor with magnetic barrier coupling," in *Proc. IEEE Int. Conf. Power Electron., Comput. Appl. (ICPECA)*, Jan. 2021, pp. 952–956.
[27] H. Du, X. Chen, G. Wen, X. Yu, and J. Lü, "Discrete-time fast terminal sliding mode control for permanent magnet linear motor," *IEEE Trans. Ind. Electron.*, vol. 65, no. 12, pp. 9916–9927, Dec. 2018.
[28] A. Besançon-Voda and P. Blaha, "Describing function approximation of a two-relay system configuration with application to Coulomb friction identification," *Control Eng. Pract.*, vol. 10, no. 6, pp. 655–668, Jun. 2002.
[29] C. Li, H. Zhao, H. Sun, and Y.-H. Chen, "Robust bounded control for nonlinear uncertain systems with inequality constraints," *Mech. Syst. Signal Process.*, vol. 140, Jun. 2020, Art. no. 106665.
[30] M. Corless and G. Leitmann, "Robust bounded control for nonlinear uncertain systems with inequality constraints," *IEEE Trans. Autom. Control*, vol. AC-26, no. 5, pp. 1139–1144, 1981.
[31] G. Leitmann, "One approach to the control of uncertain dynamical systems," *Appl. Math. Comput.*, vol. 70, nos. 2–3, pp. 261–272, Jul. 1995.
[32] H. K. Khalil, *Nonlinear Systems*, vol. 38, 2002, pp. 1091–1093.
[33] Y. H. Chen, "On the deterministic performance of uncertain dynamical systems," *Int. J. Control*, vol. 43, no. 5, pp. 1557–1579, 1986.

SHENGCHAO ZHEN (Member, IEEE) received the Ph.D. degree in mechatronic engineering from the School of Mechanical Engineering, Hefei University of Technology, Hefei, China, in 2013.

From 2011 to 2013, he was a Visiting Scholar with the George W. Woodruff School of Mechanical Engineering, Georgia Institute of Technology, Atlanta, USA, founded by China Scholarship Council. He is currently an Associate Professor with the School of Mechanical Engineering, Hefei University of Technology. His research interests include nonlinear system control theory with applications to multi-agent systems, analytic mechanics, dynamics of multibody systems, optimal control, robust control, adaptive control, fuzzy engineering, and uncertainty management.

MENG ZHANG received the B.Eng. degree in mechanical design and manufacture and automation from Nanchang University, Nanchang, China, in 2015. He is currently pursuing the M.E. degree with the School of Mechanical Engineering, Hefei University of Technology, Hefei, China.

His research interests include motion control, nonlinear system control theory with applications to manipulator control, robust control, and uncertainty management.

XIAOLI LIU received the B.E. and M.E. degrees in mechanical design and theory from the School of Mechanical Engineering, Hefei University of Technology, Hefei, China, in 2012 and 2017, respectively, where she is currently pursuing the Ph.D. degree with the School of Mechanical Engineering.

Her research interests include nonlinear system control theory with applications to motor control, analytical mechanics, multi-agent, and robotics.

HAN ZHAO received the Ph.D. degree in mechanics from Aalborg University, Denmark, in 1990.

He is currently a Professor with the School of Mechanical Engineering, Hefei University of Technology. He is also the Chief Scientist of the National Key Research and Development Program of China and the Leading Scientist of the Innovative Research Groups, National Natural Science Foundation of China. His research interests include mechanical transmission, magnetic machine, vehicles, digital design and manufacturing, information systems, dynamics, and control.

YE-HWA CHEN (Member, IEEE) received the B.S. degree in chemical engineering from the National Taiwan University, Taipei, Taiwan, and the M.S. and Ph.D. degrees in mechanical engineering from the University of California, Berkeley, CA, USA.

He is currently a Professor with the George W. Woodruff School of Mechanical Engineering, Georgia Institute of Technology, Atlanta, USA. His research interests include fuzzy dynamical systems, fuzzy reasoning, and modeling and control of mechanical systems.

XIAOFEI CHEN received the M.E. degree in control engineering from the School of Electrical Engineering, Anhui Polytechnic University, Wuhu, China, in 2017. He is currently pursuing the Ph.D. degree in mechanical engineering with the Hefei University of Technology.

His research interests include motion control, nonlinear system control theory with applications to manipulator control, robust control, and multi-agent.